ISPRS Journal of Photogrammetry and Remote Sensing 106 (2015) 95–106

Contents lists available at ScienceDirect

ISPRS Journal of Photogrammetry and Remote Sensing

journal homepage: www.elsevier.com/locate/isprsjprs

Modeling aboveground tree woody biomass using national-scale allometric methods and airborne lidar

Qi Chen *

Department of Geography, University of Hawai'i at Manoa, 422 Saunders Hall, 2424 Maile Way, Honolulu, HI 96822, USA

ARTICLE INFO

Article history:
Received 25 August 2014
Received in revised form 15 May 2015
Accepted 15 May 2015

Keywords:
Biomass
Carbon
Lidar
Allometry
Errors

ABSTRACT

Estimating tree aboveground biomass (AGB) and carbon (C) stocks using remote sensing is a critical component for understanding the global C cycle and mitigating climate change. However, the importance of allometry for remote sensing of AGB has not been recognized until recently. The overarching goals of this study are to understand the differences and relationships among three national-scale allometric methods (CRM, Jenkins, and the regional models) of the Forest Inventory and Analysis (FIA) program in the U.S. and to examine the impacts of using alternative allometry on the fitting statistics of remote sensing-based woody AGB models. Airborne lidar data from three study sites in the Pacific Northwest, USA were used to predict woody AGB estimated from the different allometric methods. It was found that the CRM and Jenkins estimates of woody AGB are related via the CRM adjustment factor. In terms of lidar-biomass modeling, CRM had the smallest model errors, while the Jenkins method had the largest ones and the regional method was between. The best model fitting from CRM is attributed to its inclusion of tree height in calculating merchantable stem volume and the strong dependence of non-merchantable stem biomass on merchantable stem biomass. This study also argues that it is important to characterize the allometric model errors for gaining a complete understanding of the remotely-sensed AGB prediction errors.

1. Introduction

Accurate spatially-explicit estimates of forest aboveground biomass (AGB) and carbon (C) stocks provide critical information for understanding and mitigating climate change (Houghton et al., 2009; Le Toan et al., 2011; Achard et al., 2014). Numerous studies have been done to map AGB using optical, radar, and lidar remote sensing data (see, e.g. Lu, 2006; Koch, 2010; Gleason and Im, 2011; Chen, 2013; Lu et al., 2014 for reviews). Along with the sheer number of studies are the often divergent AGB and C estimates from different remotely-sensed models over the same geographical area (Mitchard et al., 2014). The differences among remotely-sensed AGB estimates can be attributed to a multitude of factors including sensor and remote sensing data type, forest conditions of field plots, field plot size, statistical models, and accuracy assessment methods (Zolkos et al., 2013).

One crucial but insufficiently investigated factor that can lead to substantial AGB biomass prediction variations is the allometric model used to estimate tree biomass (Clark and Kellner, 2012). The tree biomass for calibrating a remote sensing AGB model has rarely directly *measured*; instead, it is *estimated* using allometric models with other easily measurable tree- and site-level attributes, such as DBH (diameter at breast height), tree height and wood density, as predictors (Chen et al., 2015). To estimate AGB over large spatial scales, different allometric models have been proposed over the tropics (Brown, 1997; Chave et al., 2014) and in the United States (Heath et al., 2008; Woodall et al., 2011).

In the United States, the Forest Inventory and Analysis (FIA) program of the Department of Agriculture Forest Service (USDA-FS) has developed several kinds of allometric methods to estimate AGB at the national scale. For years, FIA has used allometric models at the species- or species groups levels to estimate tree AGB within each of the FIA regional (Pacific Northwest, Interior West, Northern, and Southern) units, which hereinafter is called the regional method. Each FIA regional unit often uses different model forms (e.g., power or exponential models) and biomass predictors (e.g., some use tree height and site index while others do not) to fit AGB allometric models. The model differences sometimes reflect not necessarily the true allometry variations caused

* Tel.: +1 808 956 3524; fax: +1 808 956 3512.
E-mail address: qichen@hawaii.edu

http://dx.doi.org/10.1016/j.isprsjprs.2015.05.007
0924-2716/

by local climate, soil, and evolution history but to a large extent the personal choice of each region's model builder based on his/her knowledge and preference. This results in artifacts of biomass variations across different regions.

To alleviate this issue, Jenkins et al. (2003) did a meta-analysis of more than 2500 species-level allometric models in the literature and developed allometric models for 10 broad species groups using only one model form (i.e., power) and the same biomass predictor (i.e., DBH), hereinafter called the Jenkins method. However, since the number of species groups is small (only 10), each group is taxonomically much broader than the individual species or species groups of the regional method. So, although the Jenkins method estimates AGB consistently, it is very likely that, on a national average, it has AGB prediction errors larger than the regional method.

The Component Ratio Method (CRM) (Heath et al., 2008; Woodall et al., 2011) was proposed in recent years as an attempt to combine the strengths of both the regional and Jenkins methods. In other words, CRM is designed to integrate the national consistency from the Jenkins method and the high precision of AGB prediction from the regional method. Since 2012, the USDA-FS has used CRM instead of the Jenkins method, the conventional "gold standard" for estimating biomass, in the *Inventory of U.S. Greenhouse Gas Emissions and Sinks*.

The shift from the conventional Jenkins and regional methods to CRM has significant implications because the national biomass estimates derived from them provide critical information for the U.S. to make policies in response to global warming and climate change, especially in the intergovernmental negotiations. The choice of allometric methods affects not only the biomass estimates derived from the U.S. national forest inventory (i.e., FIA) plots (e.g., Woodbury et al., 2007; Domke et al., 2012) but also the remotely sensed biomass maps when the estimated AGB is used to calibrate remote sensing data.

In the past, the Jenkins and regional methods have been used in remote sensing studies to map biomass from local to national scales (e.g., Blackard et al., 2008; Kellndorfer et al., 2012; Zhao et al., 2012). However, few have investigated the use of CRM for remotely sensed biomass studies. Moreover, a critical analysis of CRM, especially its relationships to the Jenkins and the regional methods from which it is derived, is lacking in the literature. To my best knowledge, no research has explored the impacts of using CRM in lieu of Jenkins and regional methods on remotely-sensed AGB modeling. Thus, the main objective of this study is to use data from three study sites in the Pacific Northwest region for (1) investigating the relationships among CRM, Jenkins, and regional allometric methods and (2) exploring the impacts of the alternative allometry on the lidar-biomass model performance.

2. Study area and data

2.1. Study area

The study area encompasses a total of three sites: two in California and one in Oregon (Fig. 1). The two California sites are located on the eastern slope of the Sierra Nevada mountain range: one is the USDA-FS Sagehen Creek Experimental Forest and the other is the USDA-FS Lake Tahoe Basin Management Unit (LTBMU). The third site is the Panther Creek Watershed located in the Yamhill River Basin in western Oregon. Hereinafter, the three sites are called Sagehen, Tahoe, and Panther, respectively.

The three sites are all conifer forests, but their species compositions are different. The Sagehen site covers approximately 3925 ha, where the major species include white fir (*Abies concolor* Lindl. ex Hildebr.), red fir (*Abies magnifica* A. Murray), lodgepole pine (*Pinus contorta* Douglas ex Loudon), Jeffrey pine (*Pinus jeffreyi* Balf.), sugar pine (*Pinus lambertiana* Douglas), western white pine (*Pinus monticola* Douglas ex D. Don), and mountain hemlock (*Tsuga mertensiana* (Bong.) Carr.) (Chen et al., 2012). The Tahoe site covers about 93,598 ha, and the major vegetation is Jeffrey pine, white fir, California red fir (*Abies magnifica* A. Murray bis), lodgepole pine, incense cedar (*Calocedrus decurrens* (Torr.) Florin), quaking aspen (*Populus tremuloides* Michx.), western white pine, sugar pine, western juniper (*Juniperus occidentalis* Hook.), and mountain hemlock. The Panther site is about 2580 ha where the species is dominated by Douglas fir (*Pseudotsuga menziesii* (Mirb.) Franco), with significant amounts of red alder (*Alnus rubra* Bong.), western hemlock (*Tsuga heterophylla* (Raf.) Sarg.), western red cedar (*Thuja plicata* ex D. Don), grand fir (*Abies grandis* (Douglas ex D. Don) Lindl.), bigleaf maple (*Acer macrophyllum* Pursh) and several other species (Flewelling and McFadden, 2011) .

2.2. Forest field data

For Sagehen, field data from 80 circular plots of 12.6 m radius (0.05 ha) were used. These plots, as a part of the systematic grid of field plots measured in 2004–2006, were used to sample the forest types of the study area with 125-m spacing. The plots were located with Trimble® GeoXH™ handheld GPS with Zephyr Geodetic antenna with an average horizontal accuracy of 0.1 m. At each plot, all trees greater than 5 cm in diameter at breast height (DBH, breast height = 1.37 m) were measured with a nested sampling design. Canopy trees ($\geqslant$19.5 cm DBH) were tagged and measured in the whole plot; understory trees ($\geqslant$5 cm DBH to <19.5 cm DBH) were measured in a randomly selected third of the plot. Tree measurements include species, DBH, tree height, and vigor. A total of six vigor classes were defined that include information about whether a tree is dead or alive (Chen et al., 2012).

At Tahoe, over 1000 trees were mapped in 2012 for 56 circular plots of 17.6 m radius (0.1 ha) using a Nikon DTM-322 total station. These plots were initially established through two LTBMU projects: (1) the Multi-Species Inventory and Monitoring (MSIM) project that collected field plots on National Forest System (NFS) lands throughout the basin from 2002–2005; (2) the Lake Tahoe Urban Biodiversity (LTUB) project that established plots across multiple land ownerships at lower elevations (<7500 ft) in the basin from 2003 to 2005. Plot locations were selected using a combination of systematic/grid sampling and stratified random sampling (White and Manley, 2012). At each plot, all trees greater than 2 cm in DBH were measured. Tree measurements include species, DBH, tree height, height to live crown, and tree status (live, dead, unhealthy, or sick) (Saah et al., 2013).

The field data at Panther are from 78 circular plots of 16 m radius (0.08 ha or 0.2 acre) and were collected in the fall and winter of 2009 and spring of 2010. The field data include information about species, DBH, tree height, height to live crown, and tree status (live, cut, or dead). At each plot, all trees with DBH >0.5 cm are measured. Out of the 78 plots, 42 were established through a stratified random sample using canopy cover, canopy height, forest stand maps, hardwood percentage, crown depth indices derived from airborne lidar data collected in 2007 and NAIP (National Agriculture Imagery Program) imagery in 2005. The rest 36 plots were installed in conjunction with a soil survey, which was not dependent upon the forest conditions. Plot centers were established to an error of <0.25 m using a combination of GPS and cadastral survey (Flewelling and McFadden, 2011) (Table 1).

2.3. Airborne lidar data

The lidar data at Sagehen were collected from September 14 to 17, 2005 using an Optech ALTM 2050 system on an airplane flying

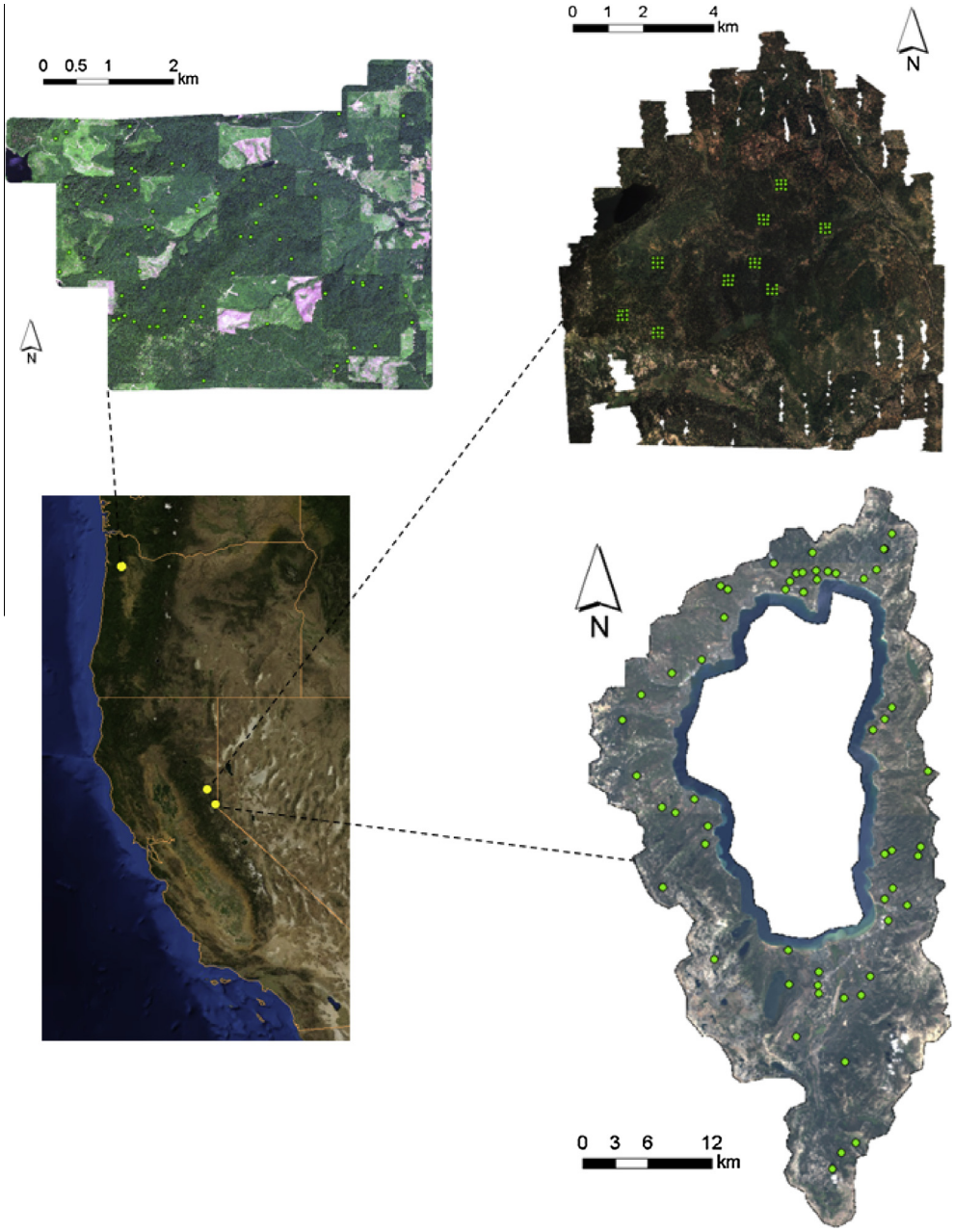

Fig. 1. Location of the three study sites: Sagehen (upper right), Tahoe (lower right), and Panther (upper left). The green dots are the locations of field plots. (For interpretation of the references to color in this figure legend, the reader is referred to the web version of this article.)

Table 1
Field plots and lidar data of the study sites.

Site	Plot number	Plot size	Plot sampling	Lidar point density (points/m^2)
Sagehen, California	80	0.05 ha	Systematic	2–4
Tahoe, California	56	0.1 ha	Systematic & stratified random	~8 or more
Panther, Oregon	78	0.08 ha	Stratified random & cadastral survey	~8 or more

at an altitude of ~800 m and average velocity of 260 km per hour. The ALTM 2050 acquired up to three returns per pulse at a pulse frequency of 50 kHz, scan frequency of 38 Hz, and a maximum scan angle of 15° from nadir, creating a swath width of ~580 m. The point density is about 2–4 returns per square meter (Chen et al., 2012).

Lidar data were acquired surrounding Lake Tahoe from August 11th to August 24th, 2010 using two Leica ALS50 Phase II laser systems mounted in a Cessna Caravan 208B. The Leica systems were set to a pulse frequency of 83–105.9 kHz, flight height of 900–1300 m, and scan angle of ±14°. The resulting point density is $\geqslant$8 pulses per square meter.

At Panther, the airborne discrete-return lidar data collected on July 15, 2010 were used, which utilized a Leica ALS60 sensor mounted in a Cessna Caravan 208B. The Leica ALS60 system was set to a pulse frequency of ⩾105 kHz, flight height of 900 m, and scan angle of ±14°. The resulting point density is also ⩾8 pulses per square meter. The airborne lidar data from both Lake Tahoe and Panther were acquired by the same company so they have similar characteristics (Table 1).

3. Methods

3.1. Individual tree biomass estimation using allometric models

The aboveground biomass of a tree includes three major components: stem, branches, and foliage. A whole tree stem can be further broken into (1) wood and bark along the horizontal dimension, or (2) merchantable stem (the portion from 1-foot stump to 4-inch top), 1-foot stump, and 4-inch top along the vertical dimension (Fig. 2). Different allometric models could use different combinations of biomass components to calculate the total biomass.

3.1.1. The Jenkins method

Jenkins et al. (2003) considered the total aboveground biomass ($B_{total,Jenkins}$) as the sum of four biomass components: merchantable stem wood ($B_{mStemWood,Jenkins}$), merchantable stem bark ($B_{mStemBark,Jenkins}$), foliage ($B_{foliage,Jenkins}$), and the other (1-foot stump, 4-inch top, and branches combined). The Jenkins method includes models of (1) $B_{total,Jenkins}$ for 10 species groups, (2) biomass fractions of merchantable stem wood, merchantable stem bark, and foliage for two vegetation types (hardwood vs. softwood). Since the regional and CRM methods do not include models for calculating foliage biomass, in this study I compared the *woody* AGB (i.e., the aboveground biomass without foliage) from the three allometric methods. For the Jenkins method, the woody AGB ($AGB_{Jenkins}$) is the difference between total aboveground biomass $B_{total,Jenkins}$ and foliage biomass $B_{foliage,Jenkins}$.

$$AGB_{Jenkins} = B_{total,Jenkins} - B_{foliage,Jenkins} \quad (1)$$

3.1.2. The regional method

The FIA PNW (Pacific Northwest Research Station) regional models (Waddell and Hiserote, 2005) calculate the woody AGB ($AGB_{regional}$) as the sum of three biomass components: total stem wood ($B_{tStemWood,regional}$), total stem bark ($B_{tStemBark,regional}$), and branches ($B_{branch,regional}$).

$$AGB_{regional} = B_{tStemWood,regional} + B_{tStemBark,regional} + B_{branch,regional} \quad (2)$$

In the FIA PNW database, $B_{tStemWood,regional}$ is calculated as the product of the CVTS (total stem wood volume from ground to tip) and wood density; CVTS is estimated using species-level models with both DBH and H as predictors. For the majority of species, $B_{tStemBark,regional}$ and $B_{branch,regional}$ are estimated using species-level models that use both DBH and H as predictors; for a few species (e.g., sugar pine, western hemlock, and western juniper), they use DBH as the only predictor. Unlike the Jenkins method, the regional method usually has different model forms for calculating the biomass components of different species.

3.1.3. The CRM method

CRM calculates the woody AGB (AGB_{crm}) as the sum of merchantable stem wood ($B_{mStemWood,crm}$), merchantable stem bark ($B_{mStemBark,crm}$), 1-foot stump ($B_{stump,crm}$), and the combination of 4-inch top and branches ($B_{topBranch,crm}$):

$$AGB_{crm} = B_{mStemWood,crm} + B_{mStemBark,crm} + B_{stump,crm} + B_{topBranch,crm} \quad (3)$$

Like the regional method, $B_{mStemWood,crm}$ and $B_{mStemBark,crm}$ are calculated as the product of merchantable stem volume and density for wood and bark, respectively. The merchantable stem bark volume is proportional to the merchantable stem wood volume. The CRM and regional methods also share the method for calculating stem wood volume. The difference is that CRM calculates merchantable stem wood volume (CV4) while the regional method

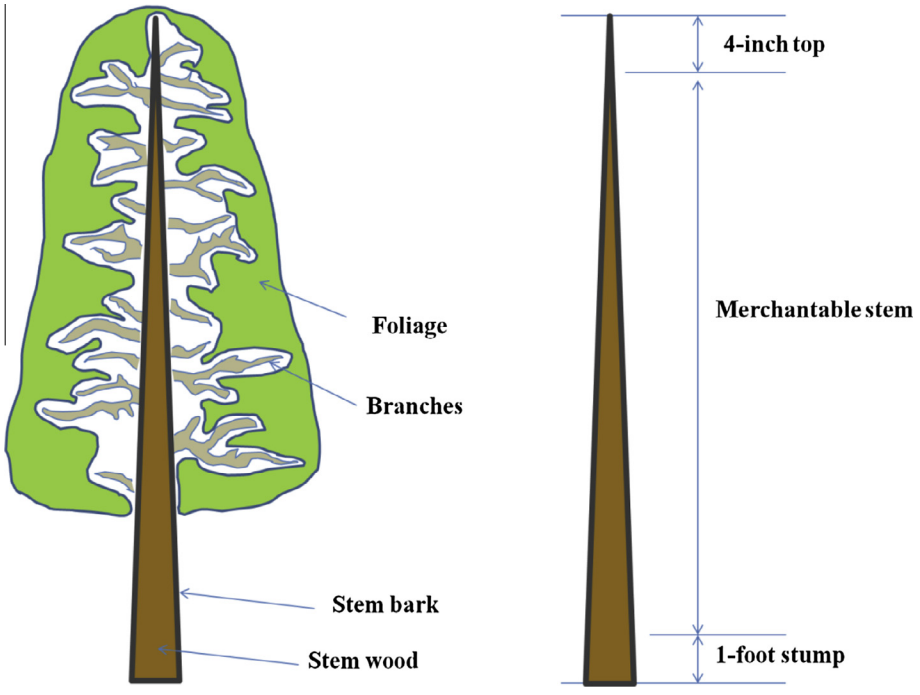

Fig. 2. Aboveground biomass components of a whole tree (left) and a tree stem (right).

calculates the total stem wood volume (CVTS). However, the two types of volumes are related: for trees of DBH ⩾12.7 cm (or 5 in.), CV4 can be calculated from CVTS through the following equations:

$$BA = 0.005454154 \times DBH^2 \quad (4)$$

$$TARIF = \frac{CVTS \times 0.912733}{1.033 \times \left(1.0 + 1.382937 \times e^{\left(4.015292 \times \frac{DBH}{10}\right)}\right) \times (BA + 0.087266) - 0.174533}$$

$$CV4 = TARIF \times (BA - 0.087266)/0.912733,$$

where CV4 and CVTS are both in cubic feet, DBH is in inches, BA is the basal area in square feet; for trees of DBH <12.7 cm, CV4 is set to 0 (Zhou and Hemstrom, 2010).

CRM calculates $B_{stump,crm}$ and $B_{topBranch,crm}$ using the following approach:

$$B_{stump,crm} = \frac{B_{mStem,crm}}{B_{mStem,Jenkins}} B_{stump,Jenkins}$$
$$B_{topBranch,crm} = \frac{B_{mStem,crm}}{B_{mStem,Jenkins}} B_{topBranch,Jenkins} \quad (5)$$

where the CRM merchantable stem biomass $B_{mStem,crm}$ is the sum of $B_{mStemWood,crm}$ and $B_{mStemBark,crm}$; the Jenkins merchantable stem biomass $B_{mStem,Jenkins}$ is the sum of $B_{mStemWood,Jenkins}$ and $B_{mStemBark,Jenkins}$; the 1-foot stump biomass $B_{stump,Jenkins}$ is calculated based on Raile (1982); and the sum of 4-inch top and branches biomass $B_{topBranch,Jenkins}$ is calculated as the difference between 1) total biomass $B_{total,Jenkins}$, and 2) the sum of foliage ($B_{foliage,Jenkins}$), merchantable stem ($B_{mStem,Jenkins}$), and stump ($B_{stump,Jenkins}$) biomass. These equations are based on the assumption that the ratio of stump or the sum of 4-inch treetop and branch biomass to merchantable stem biomass is the same for CRM and Jenkins methods. $B_{mStem,crm}/B_{mStem,Jenkins}$ is also called the CRM adjustment factor, denoted as hereinafter CRM_{AdjFac} (Woodall et al., 2011). For sapling trees of DBH <12.7 cm, the biomass AGB_{crm} is calculated as $AGB_{Jenkins}$ times the sapling adjustment factor (Woodall et al., 2011).

3.2. Calculation of biomass density at the plot level

To be consistent across the three sites, only trees of DBH >= 5 cm are considered in this analysis. The biomass of individual trees are summed within each plot and divided by the plot area to compute the biomass density at the plot level. For Sagehen that has a nested sampling design, biomass from understory trees of 5 cm <= DBH <19.5 cm is multiplied by a factor of three to calculate the total biomass within each plot. Since dead trees usually do not generate many returns from airborne lidar, only live trees are considered in our analysis (Chen et al., 2012).

3.3. Airborne lidar data processing

The airborne lidar data were processed using the Toolbox for Lidar Data Filtering and Forest Studies (Tiffs) (Chen, 2007) to (1) filter the lidar point cloud into ground returns and non-ground returns, if this had not been done when the data were delivered from lidar vendors, (2) generate DTM (Digital Terrain Model) by interpolating the ground returns to raster grids of 1 m resolution, (3) compute the canopy height of every laser point by taking the difference between its Z Cartesian coordinate and the corresponding terrain elevation, and (4) overlay the field plot boundary with the point cloud to extract the lidar metrics from the canopy height of laser points within each plot. The generated lidar metrics include mean, standard deviation, skewness, kurtosis of height, quadratic mean height, height bins at 5 m intervals, and percentile heights (10th, 20th, ... 100th percentile) (Chen et al., 2012).

3.4. Plot-level biomass statistical modeling using airborne lidar data

The impacts of allometry on lidar-biomass modeling were analyzed by developing representative regression and machine-learning models for predicting plot-level AGB density and examining their model fitting statistics. Regression models construct explicit model structure often based on a few lidar features, which are selected or transformed from a large number of lidar metrics (e.g., Lu et al., 2012; Vaglio Laurin et al., 2014; Asner and Mascaro, 2014). Machine-learning models are usually data-driven and thus produce implicit model structure (e.g., Chen and Hay, 2011; Gleason and Im, 2012; Li et al., 2014; Mascaro et al., 2014).

Based on the literature, three regression models were developed:

$$AGB = a \times H_m^b \quad (6)$$

$$AGB = a \times H_{qm}^b \quad (7)$$

$$Ln(AGB) = a \times H_{mc} + b \times CV_c + c \times CC_f \quad (8)$$

where H_m and H_{qm} are the mean and quadratic mean heights of all returns, respectively; H_{mc} and CV_c are the mean and coefficient of variance of canopy return heights, respectively; CC_f is calculated from first returns as the ratio of the numbers of canopy returns to all returns; a, b, and c are model coefficients. Canopy returns are defined as the laser returns that are higher than 1 m.

These models were chosen also because they can estimate biomass across relatively wide geographic areas and thus have good model generality (Chen, 2013). For example, the mean height has been used in boreal (Lim et al., 2003), temperate (Lefsky et al., 2002), and tropical (Asner et al., 2012; Asner and Mascaro, 2014) forests. The quadratic mean height has been used in Sagehen in a previous study (Chen et al., 2012) and in temperate forest of the eastern U.S. (Lefsky et al., 1999). Note that both H_m and H_{qm} are calculated from all returns so they incorporate information of both horizontal and vertical canopy structure (Chen, 2013; Lu et al., 2014). Model (8) was tested over three sites in Washington and Alaska by Li et al. (2008), who argued that H_{mc} and CV_c, carry information about tree height and crown depth along the vertical direction and CC_f represents canopy cover along the horizontal direction so that they can explain the majority of biomass variations. I also tried other parametric models reported from the literature (e.g., Magnussen et al., 2012), but they did not produce better performance (results not reported here) and thus were not included.

The machine-learning models chosen are support vector regression (SVR) and random forests (RF). The relationships between AGB and lidar predictors are usually nonlinear. SVR can transform the nonlinear problem into a linear one via the use of kernel functions to map the original feature space into higher dimensional space (Gunn, 1998; Smola and Schölkopf, 2004; Szuster et al., 2011). A few studies (e.g., Chen and Hay, 2011; Gleason and Im, 2012) found that SVR can outperform regression or other machine-learning algorithms for AGB modeling. In this study, the radial basis function kernel was used and the model parameters were determined by coarse- and fine-grid search similar to Chen and Hay (2011). RF is an ensemble of trees that are grown with bootstrap samples and randomly selected variables at each tree node for splitting. It is a non-parametric approach that can model complex nonlinear relationship and thus is gaining popularity in modeling AGB (e.g., Li et al., 2014; Mascaro et al., 2014). In this study, the RF parameters (the number of trees, the minimum leaf size, and the number of variables randomly selected at each node) were determined

based on the criteria of minimizing the prediction errors of the out-of-bag (oob) observations.

Five-fold cross-validation was used to produce model fitting statistics, including R^2 (coefficient of determination) and RMSE (root mean square error). Since different allometric methods could produce different AGB estimates for the same trees, the relative RMSE (RMSE divided by AGB estimates) in percentage was also calculated.

4. Results and discussion

4.1. Tree-level and plot-level AGB

Table 2 summarizes the mean tree woody AGB at each site for each allometric method. At the two California sites, on average, Jenkins has the highest AGB, followed by regional method while CRM has the smallest AGB; the means of regional and CRM AGB are about 20% and 30% less than Jenkins AGB mean, respectively. However, at Panther, CRM has the highest AGB, followed by Jenkins and regional methods; the AGB mean difference among the three allometric methods is as small as about 5–10% there.

The mean woody AGB density at the plot level follows the same pattern of mean woody AGB of individual trees among the three sites (Table 3). For example, at Sagehen, the Jenkins method produced the highest mean AGB density of 277 Mg/ha. With regional and CRM methods, the AGB density is 224 Mg/ha and 187 Mg/ha, respectively. At Panther, the highest mean AGB density is from CRM (333 Mg/ha), followed by Jenkins (313 Mg/ha) and regional (302 Mg/ha) methods. Paired t-tests indicated that, at the both tree and plot levels, the AGB between any two of the allometric models are different at the significance level of 0.05 at any of the three sites.

4.2. Revisit the CRM method and its relationship with the Jenkins method

To explain the woody AGB difference from the three allometric methods, the CRM method was revisited by combining Eqs. (3) and (5) and it was found that (see Appendix A):

$$AGB_{crm} = \frac{B_{mStem,crm}}{B_{mStem,Jenkins}} AGB_{Jenkins} \quad (9)$$

The above equation indicates that the ratio between AGB_{crm} and $AGB_{Jenkins}$ is equal to the CRM adjustment factor CRM_{AdjFac}. This not only reduces the computation of AGB_{CRM} compared to the original way introduced in Heath et al. (2008) and Woodall et al. (2011) (i.e., the method introduced in Section 3.1.3) but also concisely summarizes the relationship between woody AGB from the Jenkins and CRM methods.

Note that Eq. (9), by definition, holds for any particular tree. To examine whether this relationship can be up-scaled, the CRM and Jenkins methods were used to calculate at each site (1) the mean merchantable stem biomass of all trees (Table 2) and (2) the mean density of merchantable stem biomass of all plots (Table 3). The results show that Eq. (9) is well preserved even when individual tree biomass is averaged or summed. For example, at Panther, CRM_{AdjFac} is 1.0517 while the ratio of their mean tree-level AGB is 1.0549. Overall, negligible differences exist between the CRM_{AdjFac} and the CRM/Jenkins ratio for mean AGB at the both tree- and plot-levels (Tables 2 and 3).

In essence, it is the distribution of CRM_{AdjFac} from all trees that determines the relationship between CRM and Jenkins woody AGB estimates over an area. Fig. 3(a) shows the boxplot of CRM_{AdjFac} for trees grouped by species at Sagehen. At this site, the most dominant species is white fir (Fig. 3(b)), which has $CRM_{AdjFac} < 1$ for the majority of its trees (Fig. 3(a)). This is also true for the next three dominant species including California red fir, lodgepole pine, and Jeffrey pine. The only tree species that has average CRM_{AdjFac} greater than 1 is western white pine, but the proportion of its trees is less than 3%. The fact that the majority of trees have $CRM_{AdjFac} < 1$ at Sagehen can explain why CRM has lower than AGB estimates than Jenkins there. Likewise, at Tahoe, the most dominant tree species (Jeffrey pine, white fir, California red fir, and lodgepole pine, Fig. 3(d)) have average $CRM_{AdjFac} < 1$ (Fig. 3(c)), so CRM also produced lower AGB estimates than Jenkins. At Panther, the two most dominant species are Douglas-fir and red-alder, which consist of about 80% of all trees in the field plots (Fig. 3(f)). Their CRM_{AdjFac} medians are both slightly higher than 1 (Fig. 3(e)). This can explain that why the CRM AGB is slightly higher than Jenkins AGB estimates.

4.3. Relationship between CRM and regional methods

The CRM and regional woody AGB estimates should be closely related because (1) both the CRM and regional methods calculate stem wood biomass based on the multiplication of wood volume and density, namely the biomass expansion factor approach, (2) the merchantable wood volume (CV4) used in CRM is closely related to the total stem wood volume (CVTS) used in the regional method via Eq. (4), and (3) stem wood usually becomes the major biomass component when trees grow larger (see Figs. 5 and 6 in Jenkins et al., 2003). To confirm such a hypothesis, the relationship between CRM_{AdjFac} and $AGB_{regional}/AGB_{Jenkins}$ was analyzed and it

Table 2
Summary of tree-level AGB and merchantable stem biomass in kg at the three study sites. n is the number of trees within each site. CRM_{AdjFac} is the CRM adjustment factor.

Site	n	AGB				Merchantable stem biomass		
		Jenkins	Regional	CRM	CRM/Jenkins ratio	Jenkins	CRM	CRM_{AdjFac}
Sagehen	1898	564	456	384	0.6798	468	317	0.6773
Tahoe	924	1238	954	882	0.7123	1034	736	0.7122
Panther	3394	589	558	621	1.0549	485	510	1.0517

Table 3
Summary of plot-level AGB and merchantable stem biomass density in Mg/ha at the three study sites. n is the number of plots at each site. CRM_{AdjFac} is the CRM adjustment factor.

Site	n	AGB				Merchantable stem biomass		
		Jenkins	Regional	CRM	CRM/Jenkins ratio	Jenkins	CRM	CRM_{AdjFac}
Sagehen	80	277	224	187	0.6735	229	153	0.6660
Tahoe	56	210	162	150	0.7123	175	125	0.7122
Panther	72	313	302	333	1.0628	257	273	1.0596

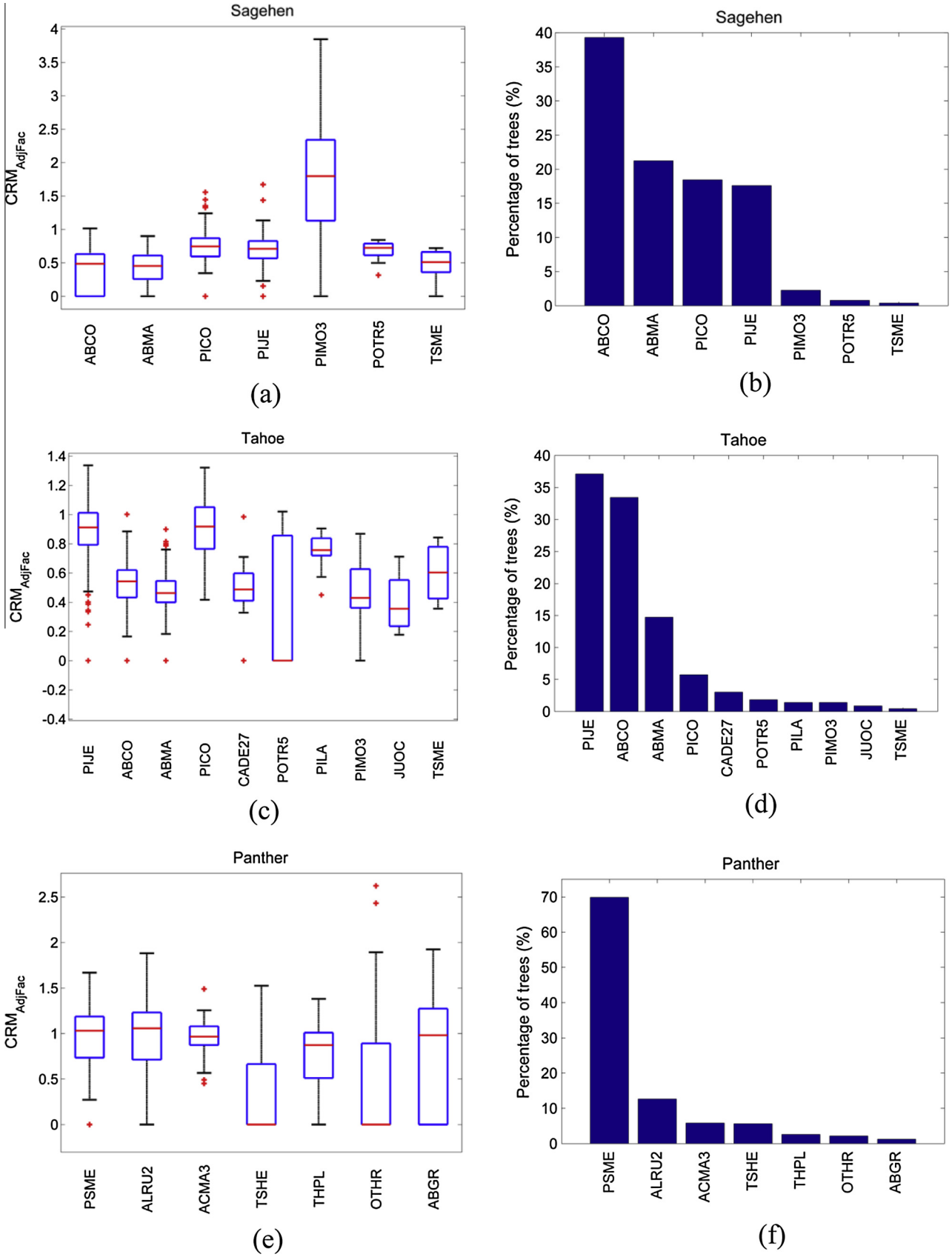

Fig. 3. CRM adjustment factor (CRM_{AdjFac}, left column) and composition (right column) of different tree species at the three study sites (Sagehen, Tahoe, and Panther). *X*-axis represents tree species with USDA PLANTS symbol:ABCO (white fir), ABMA (California red fir), ACMA3 (western hemlock), AGBR (grand fir), ALRU2 (red alder), CADE27 (incense cedar), JUOC (western juniper), PICO (lodgepole pine), PIJE (Jeffrey pine), PILA (sugar pine), PIMO3 (western white pine), POTR5 (quaking aspen), PSME (Douglas-fir), THPL (western redcedar), TSHE (bigleaf maple), and TSME (mountain hemlock). The OTHR symbol at Panther represents all species that have <1% trees within all plots. (For interpretation of the references to color in this figure legend, the reader is referred to the web version of this article.)

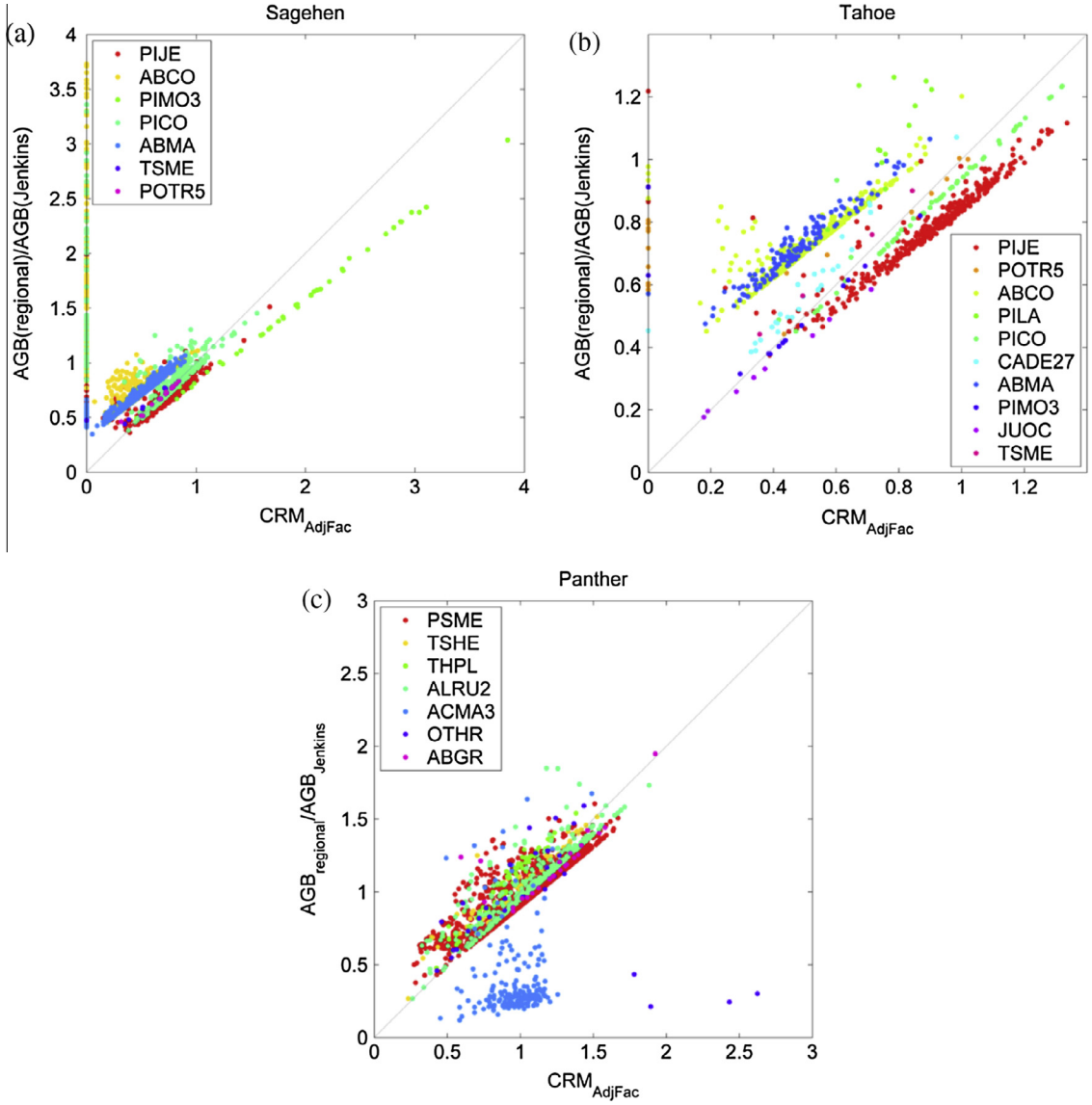

Fig. 4. Relationship between the aboveground biomass without foliage (AGB) regional/Jenkins ratio and CRM_{AdjFac} for different species. See the Fig. 3 caption for the meanings of the USDA PLANTS tree species symbols.

was found that the majority of data points are located along the 1:1 line (Fig. 4), which indicates that the two ratios are not much different from each other overall. Remember that CRM_{AdjFac} is equal to $AGB_{crm}/AGB_{Jenkins}$. This implies that, on average, AGB_{crm} and $AGB_{regional}$ should be of similar magnitude at these sites. This can explain why $AGB_{regional}$ is also much smaller than $AGB_{Jenkins}$ when AGB_{crm} is much smaller than $AGB_{Jenkins}$ at Sagehen and Tahoe (Tables 2 and 3). Note for certain species (e.g., western hemlock at Panther), the relationship CRM_{AdjFac} and $AGB_{regional}/AGB_{Jenkins}$ deviates much from the 1:1 (Fig. 4(c)). So, the ultimate relationship between CRM and regional AGB depends on both species composition and tree size distribution.

4.4. Impacts of allometry on lidar-biomass model performance

Table 4 lists the goodness-of-fit statistics of airborne lidar models for estimating plot-level woody AGB density. Overall, CRM has the best model fit, followed by the regional method while Jenkins has the worse fit. For example, when the results from all statistical methods and sites are averaged, the cross-validated R^2 for CRM, regional, and Jenkins methods is in a descending order of 0.81, 0.72, and 0.63, respectively; correspondingly, their relative RMSE increases with values of 26.4%, 33.8% and 34.3%, respectively. Note that lidar metrics are calculated mainly based on the heights of the laser points. The Jenkins method does not include tree height in their AGB estimate while the regional method does for most tree species in this study. So, it is expected that the regional woody AGB estimates can be better fitted using airborne lidar data than the Jenkins woody AGB estimates, which is consistent with the results from Zhao et al. (2012).

CRM has model fit even better than the regional method. Remember that the CRM and regional methods used the same approach for calculating stem wood biomass. So, the difference of their model fitting statistics must be attributed to the calculation of other major biomass components including stem bark and branches. For CRM, the merchantable stem bark biomass is related to the merchantable stem wood biomass through two species-specific constants (bark volume percentage and bark wood density); the branch biomass is related to the stem biomass through the Jenkins biomass fraction models, which were developed for hardwood vs. softwood. In contrast, the regional method uses species-specific and size-dependent models to calculate

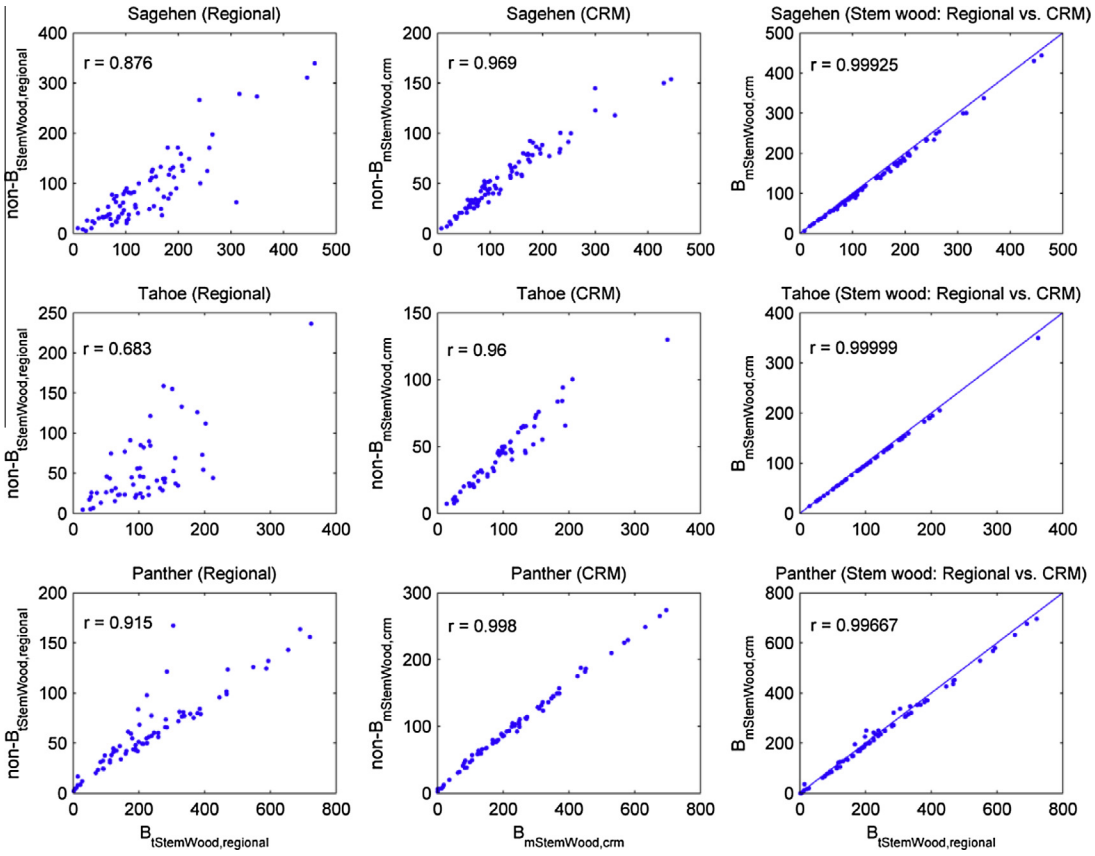

Fig. 5. (Left column) Correlation between total stem wood biomass and other biomass for the regional method; (Middle column) Correlation between merchantable stem wood biomass and other biomass for the CRM method; (Right column) Correlation between the total stem wood biomass from the regional method and the merchantable stem wood biomass from the CRM method. Correlation analysis is conducted at three study sites: Sagehen (top row), Tahoe (middle row), and Panther (bottom row).

biomass for both stem bark and branches, independent from the stem wood biomass calculation. As a result, the regional method introduces more variability in its woody AGB estimates when it sums the biomass from individual components; nevertheless, for CRM, woody AGB is highly dependent on the merchantable stem biomass. As shown in Fig. 5, the correlation between total stem wood biomass (left column, *x*-axis) and other biomass (left column, *y*-axis) for the regional method varies from 0.683 to 0.915 among the three sites. However, the correlation coefficients between merchantable stem wood biomass (middle column, *x*-axis) and other biomass (middle column, *y*-axis) for CRM are much higher and all greater than 0.96. All these, combining with the fact that the regional total stem wood biomass and CRM merchantable stem wood biomass has almost 1:1 relationship (right column), can explain why CRM has the best fit for the lidar-based biomass models.

The impacts of allometry on lidar model performance vary with sites and are substantial sometimes (Table 4). At Panther, different allometric methods have relatively small differences in fitting statistics. At Sagehen, the model fitting statistics from different allometric methods have larger yet moderate difference. However, at Tahoe, the difference in model fitting statistics from the three allometric methods is striking: for instance, the R^2 is only 0.41–0.57 for the Jenkins method while it is as high as 0.77–0.92 for CRM. Since Jenkins has DBH as the only predictor while lidar mainly carries height information, the poor performance from Jenkins at this site could be related to the loose relationship between DBH and height there. This is confirmed by the results that, when a simple power model was used to fit individual tree height based on DBH, the R^2 is only 0.6 at Saghen, in contrast to 0.82 at the other two sites (Fig. 6).

4.5. Need for characterizing allometric model errors

Characterizing the AGB prediction errors have become one of the central topics in remote sensing of forest biomass and C. A rigorous assessment of the remotely sensed AGB prediction errors should consider errors in the whole process of biomass estimation, including errors in field measurements, allometry, remote sensing data (e.g., imperfect geometric and atmospheric corrections), and remote sensing model errors. Chen et al. (2015) proposed a new framework of characterizing AGB predicting errors by comprehensively considering these different error sources and propagating the errors from trees to field plots and finally to pixel levels for a tropical forest in Ghana. It was found that the AGB prediction errors are dominated by the errors from allometric models and remote sensing models.

The error statistics reported in this study, RMSE and relative RMSE, are to characterize the remote sensing model errors only, assuming that the allometric models are free of errors. This is an unrealistic but widely used assumption in the literature. However, without considering other errors, especially the allometric model errors, it is hard to gain a complete understanding of the whole AGB prediction errors. For example, in this study, CRM produced the lowest lidar-AGB model errors. Nevertheless, it is still unclear whether CRM is the best allometric method for biomass estimation. This is because, if the allometric model used to estimate tree biomass has large errors, the errors of the remotely-sensed AGB estimates could also be large, even in the case that the remote sensing biomass model has small errors.

The characterization of allometric model errors requires destructively measured AGB of individual trees (Clark and Kellner, 2012). Unfortunately, the destructively measured tree

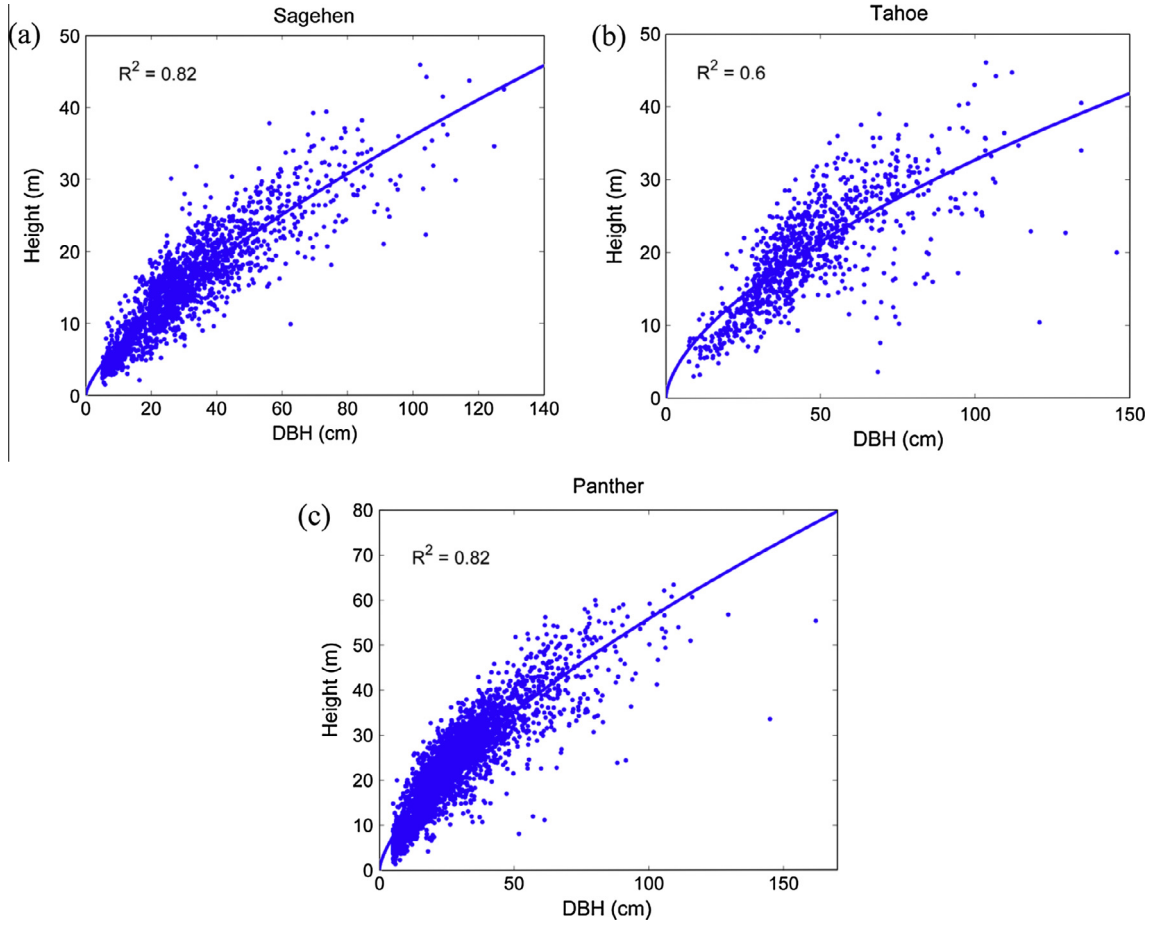

Fig. 6. Relationship between individual tree DBH and height at the three study sites (Sagehen, Tahoe, and Panther). The data at each site are fitted using a simple power model (thick line) with the coefficient of determination (R^2) labelled.

Table 4
Cross-validation fitting statistics of lidar-biomass models based on different allometric methods (Jenkins, regional, and CRM) and different statistical methods ($f(H_{qm})$: Eq. (6); $f(H_m)$: Eq. (7); Li08: Eq. (8); SVR: support vector regression; RF: random forest).

	R^2			RMSE (Mg/ha)			Relative RMSE (%)		
	Jenkins	Regional	CRM	Jenkins	Regional	CRM	Jenkins	Regional	CRM
Sagehen									
$f(H_{qm})$	0.66	0.75	0.77	97.6	76.8	56.0	35.2%	34.2%	30.0%
$f(H_m)$	0.53	0.58	0.62	115.2	98.6	71.4	41.6%	43.9%	38.2%
Li08	0.69	0.78	0.78	93.6	71.5	54.4	33.8%	31.9%	29.1%
SVR	0.65	0.76	0.75	98.8	75.5	58.1	35.7%	33.7%	31.1%
RF	0.49	0.66	0.62	119.8	88.6	72.1	43.2%	39.5%	38.6%
Tahoe									
$f(H_{qm})$	0.51	0.63	0.92	75.1	58.3	23.6	35.8%	36.0%	15.7%
$f(H_m)$	0.54	0.64	0.91	72.6	57.5	24.1	34.6%	35.6%	16.1%
Li08	0.48	0.60	0.89	77.1	60.5	27.5	36.7%	37.4%	18.4%
SVR	0.57	0.66	0.91	70.4	55.8	24.5	33.5%	34.5%	16.4%
RF	0.41	0.56	0.77	82.2	63.5	39.0	39.1%	39.2%	26.0%
Panther									
i(H_{qm})	0.80	0.83	0.85	90.8	82.8	87.2	29.0%	27.4%	26.2%
$f(H_m)$	0.79	0.82	0.84	92.9	85.9	89.9	29.7%	28.5%	27.0%
Li08	0.80	0.84	0.85	89.6	81.8	86.5	28.6%	27.1%	26.0%
SVR	0.81	0.84	0.85	87.2	81.4	86.5	27.9%	27.0%	26.0%
RF	0.78	0.78	0.79	94.9	95.6	104.3	30.3%	31.7%	31.3%
Average	0.63	0.72	0.81	90.5	75.6	60.3	34.3%	33.8%	26.4%

AGB data that were used to develop those published allometric models are usually inaccessible to users. The error information (e.g., RMSE) of allometric models, especially those developed tens of years ago, was not necessarily reported in the literature either. This is particularly the case for the species-level allometric models of the regional method. Among the three allometric methods

investigated in this study, the Jenkins method is the only one that has reported the allometric model errors (Jenkins et al., 2004). However, their allometric model RMSEs were calculated based on "pseudodata" generated from published equations instead of real tree AGB measurements, which causes an underestimation of the true allometric model errors (Chen et al., 2015).

Compiling and collecting measurements of tree AGB across large spatial scales are a mammoth undertaking, so a national database of tree AGB measurements for species in the U.S. does not exist yet. Nevertheless, for quantifying national scale AGB and its uncertainty in a creditable manner, such works need to be done in the future. Chave et al. (2014) recently developed a pan-tropical tree AGB database, based on which the errors related to allometric model can be thoroughly investigated and the errors related to remote sensing AGB prediction can be well characterized (Chen et al., 2015). Similar efforts should be among the top research priorities of the U.S. and other nations to estimate and map AGB at the large spatial scale.

5. Conclusions

Allometry plays a fundamental role in biomass estimation and remotely sensed biomass mapping. CRM, a national-scale allometric method in the U.S., has been recently proposed by the USDA-FS FIA program for biomass and C stock inventory. Using data from three conifer forests in the Pacific Northwest, this study a) conducted an in-depth of analysis of CRM and two other national-scale allometric methods (Jenkins and regional methods) from which CRM is derived, and b) compared the use of the three allometric methods for biomass estimation and lidar-based AGB modeling. It was found that:

(1) In terms of biomass estimation, the difference of woody AGB estimates between CRM and the Jenkins method is attributed to their merchantable stem wood biomass estimate differences. The woody AGB estimates from CRM and the regional method is closely related because they share the approach of calculating stem wood biomass. The relative magnitude of AGB estimates from the three allometric methods varies, depending on species composition and tree size distribution at each site.
(2) In terms of biomass modeling, CRM produced the lowest errors for the lidar-based biomass models, while Jenkins led to the largest lidar-biomass model errors. The poor lidar biomass model performance from Jenkins is mainly related to its exclusion of tree height in their biomass estimation. The superior performance of CRM is largely attributed to its simple way of calculating non-merchantable-stem biomass. At a given site, the variation of lidar-based AGB model errors across different allometric methods is driven by the extent to which how closely tree DBH and height are correlated.

The implications of this study are multifold. First, despite CRM has the best lidar-AGB model fitting, it has deep roots in the simplification of calculating non-merchantable-stem biomass and thus has the concern of being just a mathematical artifact. A pressing need exists to create a national database of tree AGB measurements for evaluating the errors of CRM or other national allometric methods and, eventually, even develop new allometric methods that can estimate AGB consistently across the nation and characterize errors rigorously. Second, since the use of different allometric methods at a given site could cause substantial variations in lidar-AGB model performance, the interpretation of remotely-sensed biomass model performance should be always put in the context of the allometric method used. For example, it is inappropriate to directly compare the remote sensing AGB model performance (e.g., R^2) in Africa and the U.S. without considering the differences in their allometric model errors.

The study also tested five different statistical methods (three regression models and two machine learning methods) for AGB modeling. RF was the worst method for almost every allometric method at each of three study sites. This is in contrast to some previous studies such as Li et al. (2014) and Mascaro et al. (2014), who reported superior results of using RF in temperate and tropical forests. RF is essentially a tree-based approach and at each leaf node the model prediction is an average of training data values within it, which tends to underestimate high AGB areas and overestimate low AGB areas. Such a problem is more obvious if cross-validation is used for model assessment, in which the dynamic range of AGB of the test data could be larger than the one of the training data. So, it is not unexpected that RF had the largest errors (RMSE) in this study. However, the three study sites here are all conifer forests. More research is needed in the future to compare different statistical models across different forest types.

Acknowledgements

The data at Panther were made available through the Panther Creek Cooperative Research Project. The data collection at Tahoe was funded by the Southern Nevada Public Lands Management Act. Great thanks are extended to Dr. Jim Flewelling, Mr. Travis Freed, Dr. David Saah, Dr. Jason Moghaddas, and Dr. John Battles in collecting and/or sharing the data.

Appendix A

The derivation of woody AGB relationship between CRM and Jenkins methods.

$$
\begin{aligned}
&AGB_{crm} = B_{mStemWood,crm} + B_{mStemBark,crm} + B_{mStem,crm} \\
&\times (B_{stump,Jenkins}/B_{mStem,Jenkins}) + B_{mStem,crm} \times (B_{topBranch,Jenkins}/B_{mStem,Jenkins}) \\
&= B_{mStem,crm} + B_{mStem,crm} \times (B_{stump,Jenkins}/B_{mStem,Jenkins}) + B_{mStem,crm} \\
&\times (B_{topBranch,Jenkins}/B_{mStem,Jenkins}) \\
&= (B_{mStem,Jenkins} + B_{stump,Jenkins} + B_{topBranch,Jenkins}) \\
&\times (B_{mStem,crm}/B_{mStem,Jenkins}) \\
&= (B_{total,Jenkins} - B_{foliage,Jenkins}) \times (B_{mStem,crm}/B_{mStem,Jenkins}) \\
&= AGB_{Jenkins} \times (B_{mStem,crm}/B_{mStem,Jenkins})
\end{aligned}
$$

References

Achard, F., Beuchle, R., Mayaux, P., Stibig, H.J., Bodart, C., Brink, A., Carboni, S., Desclée, B., Donnay, F., Eva, H., Lupi, A., Raši, R., Seliger, R., Simonetti, D., 2014. Determination of tropical deforestation rates and related carbon losses from 1990 to 2010. Glob. Change Biol. 20 (8), 2540–2554.

Asner, G.P., Mascaro, J., 2014. Mapping tropical forest carbon: calibrating plot estimates to a simple LiDAR metric. Remote Sens. Environ. 140, 614–624.

Asner, G.P., Mascaro, J., Muller-Landau, H.C., Vieilledent, G., Vaudry, R., Rasamoelina, M., Hall, J.S., van Breugel, M., 2012. A universal airborne LiDAR approach for tropical forest carbon mapping. Oecologia 168 (4), 1147–1160.

Blackard, J.A., Finco, M.V., Helmer, E.H., Holden, G.R., Hoppus, M.L., Jacobs, D.M., Lister, A.J., Moisten, G.G., Nelson, M.D., Riemann, R., Ruefenacht, B., Salajanu, D., Weyermann, D.L., Winterberger, K.C., Brandeis, T.J., Czaplewski, R.L., McRoberts, R.E., Patterson, P.L., Tymcio, R.P., 2008. Mapping US forest biomass using nationwide forest inventory data and moderate resolution information. Remote Sens. Environ. 112 (4), 1658–1677.

Brown, S., 1997. Estimating biomass and biomass change of tropical forests: a primer, vol. 134. Food & Agriculture Organization.

Chave, J., Réjou-Méchain, M., Búrquez, A., Chidumayo, E., Colgan, M.S., Delitti, W.B., Duque, A., Eid, T., Fearnside, P.M., Goodman, R.C., Henry, M., Martínez-Yrízar, A., Mugasha, W.A., Muller-Landau, H.C., Mencuccini, M., Nelson, B.W., Ngomanda, A., Nogueira, E.M., Ortiz-Malavassi, E., Pélissier, R., Ploton, P., Ryan, C.M., Saldarriaga Martinze, J.G., Vieilledent, G., 2014. Improved allometric models to estimate the aboveground biomass of tropical trees. Glob. Change Biol. http://dx.doi.org/10.1111/gcb.12629.

Chen, Q., 2007. Airborne lidar data processing and information extraction. Photogramm. Eng. Remote Sens. 73 (2), 109.
Chen, Q., 2013. Lidar remote sensing of vegetation biomass. In: Weng, Q., Wang, G. (Eds.), Remote Sensing of Natural Resources. CRC Press, Taylor & Francis Group.
Chen, G., Hay, G.J., 2011. A support vector regression approach to estimate forest biophysical parameters at the object level using airborne lidar transects and quickbird data. Photogramm. Eng. Remote Sens. 77 (7), 733–741.
Chen, Q., Vaglio Laurin, G., Battles, J.J., Saah, D., 2012. Integration of airborne lidar and vegetation types derived from aerial photography for mapping aboveground live biomass. Remote Sens. Environ. 121, 108–117.
Chen, Q., Vaglio Laurin, G., Valentini, R., 2015. Uncertainty of remotely sensed aboveground biomass over an African tropical forest: propagating errors from trees to plots to pixels. Remote Sens. Environ. 160, 134–143.
Clark, D.B., Kellner, J.R., 2012. Tropical forest biomass estimation and the fallacy of misplaced concreteness. J. Veg. Sci. 23 (6), 1191–1196.
Domke, G.M., Woodall, C.W., Smith, J.E., Westfall, J.A., McRoberts, R.E., 2012. Consequences of alternative tree-level biomass estimation procedures on US forest carbon stock estimates. For. Ecol. Manage. 270, 108–116.
Flewelling, J.W., McFadden, G., 2011. LiDAR data and cooperative research at Panther Creek, Oregon. In: Proceedings of SilviLaser, Hobart, Austria, October 16–20, 2011.
Gleason, C.J., Im, J., 2011. A review of remote sensing of forest biomass and biofuel: options for small-area applications. GISci. Remote Sens. 48 (2), 141–170.
Gleason, C.J., Im, J., 2012. Forest biomass estimation from airborne LiDAR data using machine learning approaches. Remote Sens. Environ. 125, 80–91.
Gunn, S.R., 1998. Support vector machines for classification and regression. ISIS Technical Report, 14.
Heath, L.S., Hansen, M., Smith, J.E., Miles, P.D., Smith, B.W., 2008. Investigation into calculating tree biomass and carbon in the FIADB using a biomass expansion factor approach. In: W. McWilliams, G. Moisen, R. Czaplewski (Eds.), Proceedings of the Annual Forest Inventory and Analysis Symposium, Park City, Utah, October 21–23, 2008. RMRS-P-56CD. U.S. Department of Agriculture, Forest Service, Rocky Mountain Research Station, Fort Collins, CO. 26 p.
Houghton, R.A., Hall, F., Goetz, S.J., 2009. Importance of biomass in the global carbon cycle. J. Geophys. Res.: Biogeosci., 114 http://dx.doi.org/10.1029/2009JG000935, G00E03.
Jenkins, J.C., Chojnacky, D.C., Heath, L.S., Birdsey, R.A., 2003. National-scale biomass estimators for United States tree species. Forest Sci. 49 (1), 12–35.
Jenkins, J.C., Chojnacky, D.C., Heath, L.S., Birdsey, R.A., 2004. Comprehensive database of diameter-based biomass regressions for North American tree species. Gen. Tech. Rep. NE-319. Newtown Square, PA: U.S. Department of Agriculture, Forest Service, Northeastern Research Station. 45 p.
Kellndorfer, J., Walker, W., LaPoint, E., Bishop, J., Cormier, T., Fiske, G., Hoppus, M., Kirsch, K., Westfall, J. 2012. NACP Aboveground Biomass and Carbon Baseline Data (NBCD 2000), U.S.A., 2000. Data set. <http://daac.ornl.gov> from ORNL DAAC, Oak Ridge, Tennessee, U.S.A. <http://dx.doi.org/10.3334/ORNLDAAC/1081>.
Koch, B., 2010. Status and future of laser scanning, synthetic aperture radar and hyperspectral remote sensing data for forest biomass assessment. ISPRS J. Photogramm. Remote Sens. 65, 581–590.
Le Toan, T., Quegan, S., Davidson, M.W.J., Balzter, H., Paillou, P., Papathanassiou, K., Plummer, S., Rocca, F., Saatchi, S., Shugart, H., Ulander, L., 2011. The BIOMASS mission: mapping global forest biomass to better understand the terrestrial carbon cycle. Remote Sens. Environ. 115 (11), 2850–2860.
Lefsky, M.A., Harding, D., Cohen, W.B., Parker, G., Shugart, H.H., 1999. Surface lidar remote sensing of basal area and biomass in deciduous forests of eastern Maryland, USA. Remote Sens. Environ. 67 (1), 83–98.
Lefsky, M.A., Cohen, W.B., Harding, D.J., Parker, G.G., Acker, S.A., Gower, S.T., 2002. Lidar remote sensing of above-ground biomass in three biomes. Glob. Ecol. Biogeogr. 11 (5), 393–399.
Li, Y., Andersen, H.E., McGaughey, R., 2008. A comparison of statistical methods for estimating forest biomass from light detection and ranging data. Western J. Appl. Forestry 23 (4), 223–231.
Li, M., Im, J., Quackenbush, L.J., Liu, T., 2014. Forest biomass and carbon stock quantification using airborne lidar data: a case study over huntington wildlife forest in the adirondack park. IEEE J. Selected Topics Appl. Earth Observ. Remote Sens. 7, 3143–3156.
Lim, K., Treitz, P., Baldwin, K., Morrison, I., Green, J., 2003. Lidar remote sensing of biophysical properties of tolerant northern hardwood forests. Can. J. Remote Sens. 29 (5), 658–678.
Lu, D., 2006. The potential and challenge of remote sensing-based biomass estimation. Int. J. Remote Sens. 27, 1297–1328.
Lu, D., Chen, Q., Wang, G., Moran, E., Batistella, M., Zhang, M., Vaglio Laurin, G., Saah, D., 2012. Aboveground forest biomass estimation with Landsat and lidar data and uncertainty analysis of the estimates. Int. J. Forestry Res. Article ID 436537.
Lu, D., Chen, Q., Wang, Liu, L., Li, G., Moran, E., 2014. A survey of remote sensing-based aboveground biomass estimation methods in forest ecosystems. Int. J. Digital Earth. http://dx.doi.org/10.1080/17538947.2014.990526.
Magnussen, S., Næsset, E., Gobakken, T., Frazer, G., 2012. A fine-scale model for area-based predictions of tree-size-related attributes derived from LiDAR canopy heights. Scand. J. For. Res. 27 (3), 312–322.
Mascaro, J., Asner, G.P., Knapp, D.E., Kennedy-Bowdoin, T., Martin, R.E., Anderson, C., Higgins, M., Chadwick, K.D., 2014. A tale of two "forests": random forest machine learning aids tropical forest carbon mapping. PLoS ONE 9 (1), e85993.
Mitchard, E.T., Feldpausch, T.R., Brienen, R.J., Lopez-Gonzalez, G., Monteagudo, A., Baker, T.R., Pardo Molina, G., 2014. Markedly divergent estimates of Amazon forest carbon density from ground plots and satellites. Glob. Ecol. Biogeogr. 23, 935–946.
Saah, D., Moody, T., Moghaddas, J., Collins, B., Freed, T., Chen, Q., O'Neil-Dunne, J., Johnson, G., Moghaddas, E., 2013. A condition assessment of fire hazard and risk in the wildland urban interface (WUI) and stream environment zones (SEZ's) of the Lake Tahoe Basin. Project Report for the Pacific Southwest Research Station.
Smola, A.J., Schölkopf, B., 2004. A tutorial on support vector regression. Statist. Comput. 14 (3), 199–222.
Szuster, B.W., Chen, Q., Borger, M., 2011. A comparison of classification techniques to support land cover and land use analysis in tropical coastal zones. Appl. Geography 31 (2), 525–532.
Vaglio Laurin, G., Chen, Q., Lindsell, J.A., Coomes, D.A., Frate, F.D., Guerriero, L., Pirotti, F., Valentini, R., 2014. Above ground biomass estimation in an African tropical forest with lidar and hyperspectral data. ISPRS J. Photogramm. Remote Sens. 89, 49–58.
Waddell, K.L., Hiserote, B., 2005. The PNW-FIA Integrated Database User Guide and Documentation: Version 2.0, Forest Inventory and Analysis Program. Pacific Northwest Research Station, Portland, OR.
White, A., and Manley, P., 2012. Wildlife habitat occurrence models for project and landscape evaluations in the Lake Tahoe basin. Final Report to the U.S. Department of Interior, Bureau of Land Management.
Woodall, C.W., Heath, L.S., Domke, G.M., Nichols, M.C., 2011. Methods and equations for estimating aboveground volume, biomass, and carbon for trees in the US forest inventory, 2010. Gen. Tech. Rep. NRS-88. Newtown Square, PA: U.S. Department of Agriculture, Forest Service, Northern Research Station.
Woodbury, P.B., Smith, J.E., Heath, L.S., 2007. Carbon sequestration in the US forest sector from 1990 to 2010. For. Ecol. Manage. 241 (1), 14–27.
Zhao, F., Guo, Q., Kelly, M., 2012. Allometric equation choice impacts lidar-based forest biomass estimates: a case study from the Sierra National Forest, CA. Agric. For. Meteorol. 165, 64–72.
Zhou, X.P., Hemstrom, M.A., 2010. Timber volume and aboveground live tree biomass estimations for landscape analyses in the Pacific Northwest. Gen. Tech. Rep. PNW-GTR-819. Portland, OR: U.S. Department of Agriculture, Forest Service, Pacific Northwest Research Station.
Zolkos, S.G., Goetz, S.J., Dubayah, R., 2013. A meta-analysis of terrestrial aboveground biomass estimation using lidar remote sensing. Remote Sens. Environ. 128, 289–298.